PNAS RESEARCH ARTICLE | AGRICULTURAL SCIENCES

A universal design of restructured dimer antigens: Development of a superior vaccine against the paramyxovirus in transgenic rice

Fanshu Ma[a,b,c,d,e,1], Qianru Xu[f,1], Aiping Wang[d], Daichang Yang[g], Qingmei Li[h], Junqing Guo[h], Longxian Zhang[a,c], Jiquan Ou[i], Rui Li[h], Heng Yin[i], Kunpeng Li[i], Li Wang[h], Yanan Wang[h], Xiangyue Zhao[h], Xiangxiang Niu[a], Shenli Zhang[a], Xueyang Li[a], Shujun Chai[h], Erqin Zhang[a,c,2], Zihe Rao[j,2], and Gaiping Zhang[a,b,c,d,2]

Edited by Roy Curtiss III, University of Florida, Gainesville, FL; received June 9, 2023; accepted December 5, 2023

The development of vaccines, which induce effective immune responses while ensuring safety and affordability, remains a substantial challenge. In this study, we proposed a vaccine model of a restructured "head-to-tail" dimer to efficiently stimulate B cell response. We also demonstrate the feasibility of using this model to develop a paramyxovirus vaccine through a low-cost rice endosperm expression system. Crystal structure and small-angle X-ray scattering data showed that the restructured hemagglutinin–neuraminidase (HN) formed tetramers with fully exposed quadruple receptor binding domains and neutralizing epitopes. In comparison with the original HN antigen and three traditional commercial whole virus vaccines, the restructured HN facilitated critical epitope exposure and initiated a faster and more potent immune response. Two-dose immunization with 0.5 μg of the restructured antigen (equivalent to one-127th of a rice grain) and one-dose with 5 μg completely protected chickens against a lethal challenge of the virus. These results demonstrate that the restructured HN from transgenic rice seeds is safe, effective, low-dose useful, and inexpensive. We provide a plant platform and a simple restructured model for highly effective vaccine development.

structural vaccine | transgenic rice | BCR | paramyxovirus

Significance

The "ideal vaccine" should accurately induce immune responses without strain on the immune system. It should be readily scaled up for bulk manufacture and be easily stored and transported. To achieve this, a "head-to-tail" model was proposed to mimic the natural structure of protective antigen in paramyxovirus. The restructured HN (hemagglutinin–neuraminidase) facilitated epitope exposure while also initiating a faster and more potent immune response. Remarkably, two-dose immunization with 0.5 μg of the restructured HN (equivalent to one-127th of a rice grain) completely protected chickens against a lethal challenge, highlighting the public health value of restructured HN as a superior immunogen.

For more than a century, vaccines have made a significant contribution to the control of infectious diseases (1). Through vaccination, the morbidity and mortality rates of tetanus, measles, polio, mumps, rubella, pneumococci, and hepatitis B have been reduced by 97 to 99% (2, 3). Vaccination has arguably been the most cost-effective public health measure of the past century. For every US dollar invested in immunization, there is an estimated $16 in health care savings and increased economic productivity (World Health Organization) (4). Since its inception, vaccines have relied almost exclusively on empirical, trial-and-error methods that attempt to mimic the process of natural infection while reducing adverse reactions to acceptable levels (5). Advancements in basic immunology, coupled with the ready access to atomic-level structural data for viral surface proteins, have greatly facilitated the design of vaccine immunogens. This process has evolved into a protein engineering exercise, which is now less uncertain compared to using biological agents (6).

Conventional vaccines against pathogens are currently available in three forms: killed virulent pathogens, attenuated live vaccines, and major components of pathogens (3). The first generation of whole virus vaccines relied on empirical attenuation, but their classical attenuation process remains unpredictable. International trade and biosafety concerns, including the risk of reversion to wild-type virulence and potential harm to individuals with impaired immunity, have limited the use of whole virus vaccines. As a result, there has been a shift toward the use of major components of pathogens as vaccines (7, 8). The second generation of subunit vaccines, characterized by recombinant products with well-defined molecular structures, has become a focus of vaccine development (9). Examples of subunit vaccines include the hepatitis B vaccine and pneumonia vaccine. However, this strategy has not universally achieved success, as expressing original proteins as immunogens often fails to generate sufficient protective immune responses. The limited efficacy is attributed to the inability of soluble protein monomers to efficiently activate the immune system (10, 11).

The B cell antigen receptor (BCR) is one of the most abundant receptors. Previous studies have confirmed that efficient cross-linking of BCRs is an important step in the early stages of B cell activation (12–14). Multivalent antigens with identical epitopes are capable of triggering B cell cross-linking and T cell–independent IgM responses (15), whereas soluble proteins do not elicit adequate immune responses (16, 17). To address

Competing interest statement: Authors J.O., H.Y., and K.L. were employed by the company Wuhan Healthgen Biotechnology Corp., Wuhan, China. The remaining authors declare that the research was conducted in the absence of any commercial or financial relationships that could be construed as a potential conflict of interest.

This article is a PNAS Direct Submission.

[1]F.M. and Q.X. contributed equally to this work.

[2]To whom correspondence may be addressed. Email: zhangerqin76@163.com, raozh@mail.tsinghua.edu.cn, or zhanggaiping2003@163.com.

This article contains supporting information online at https://www.pnas.org/lookup/suppl/doi:10.1073/pnas.2305745121/-/DCSupplemental.

Published January 18, 2024.

this problem, the immunogenicity of soluble proteins has previously been enhanced by constructing virus-like particles (VLP) and structure-based epitope vaccines (6). These self-assembled antigens display multiple repetitive epitopes and form large particles to improve immunogenicity. Although self-assembled vaccines have been successfully applied to control the disease caused by human papillomavirus, VLPs still have certain limitations. For example, VLPs are not always stable. VLPs require a strict high ion solution for structural integrity, yet may cause side effects (18, 19). Therefore, it is necessary to find other methods to change the antigen conformation and improve the immunogenicity of subunit vaccines.

Viruses in the Family *Paramyxoviridae* are enveloped, negative-sense, and contain single-stranded RNA, which have been shown to infect both humans and animals. Viruses in this family include mumps virus, measles virus, parainfluenza virus 1 to 5, canine distemper virus, Newcastle disease virus (NDV), Nipah virus, and Hendra virus. During the process of infection, nearly all paramyxoviruses must fuse their lipid envelopes with host cell membranes in a receptor-dependent, pH-independent manner (20). For most members of the *Paramyxoviridae* family, membrane fusion and entry are mediated by two spike glycoproteins in the lipid membrane, an attachment protein referred to as hemagglutinin–neuraminidase (HN) or hemagglutinin (H) or glycoprotein (G) (depending on the virus), and Fusion (F) protein (21). Both HN/H/G and F proteins play pivotal roles in inducing the production of virus-neutralizing antibodies, rendering them promising antigens for subunit vaccine development. We have previously endeavored to develop a subunit vaccine centered around the F protein; however, it did not confer complete protection at low doses (22). The HN protein is a type II membrane protein consisting of an N-terminal transmembrane domain (TM) followed by a stalk region and an enzymatically active neuraminidase (NA) (23, 24). This protein plays multiple roles in viral entry and egress (25, 26). On the surface of the virus, HN protein is present as a tetramer. HN tetramer plays an important role in the immunological activity and process of membrane fusion (27–29). The structural stability of the HN tetramer relies on disulfide bonds and noncovalent bonds. However, it is important to note that the extracellular region of the HN protein alone cannot form a stable tetramer (30–32). Despite the presence of a cysteine at position 123 of HN, which forms an interchain disulfide bond, it is not sufficient to confer stability to the tetramer. Previously, attempts have been made to develop vaccines based on the HN protein, but satisfactory results have not been achieved (33, 34). Consequently, there are currently no commercialized subunit vaccines available.

The "ideal vaccine" should be effective, safe, and inexpensive without strain on the immune system. It should be readily scaled up for bulk manufacture and should be stored and transported easily. In addition, the ideal vaccine should accurately induce an effective immune response with a low vaccination dose. To achieve this goal, a vaccine antigen model is proposed using a "head-to-tail" dimer stably connected by covalent bonds (Fig. 1*A*). The restructured antigen displays multiple pairs of identical epitopes with appropriate distance to effectively activate B cells. In this study, the receptor-binding protein of NDV in the Family *Paramyxoviridae* was selected as an example to restructure a dimer antigen with a flexible linker. The restructured HN protein was expressed in rice endosperm to obtain low-cost eukaryotic antigens. The structure of protein folding was confirmed by solution SAXS (small-angle X-ray scattering) analysis and X-ray crystallography. Immunoassays and protective assays demonstrated that the antigen design significantly enhanced the immune response of subunit vaccines with higher antibody titers. An immunization dose at the nanogram level completely protected chickens against lethal virus infection. This extremely low-dose vaccine effectively activated B cells and greatly reduced the side effects associated with vaccination.

Results

Design and Screening Osr2HN Stably Expressed in the Transgenic Rice Endosperm. The rice endosperm system is a promising eukaryotic expression vehicle for obtaining stable recombinant proteins. Rice seeds offer advantages such as long-term storage capability and scalable production, making them suitable for efficient antigen production for vaccine development (35–37). Therefore, a tandem *Oryza sativa* recombinant HN protein (Osr2HN) was constructed and linked by a (GGGGS)3 linker based on the expression system of transgenic rice seeds. In addition, an *O. sativa* recombinant HN monomer (OsrHN) was constructed as a control. In order to obtain a high expression level in rice seeds, the tandem HN protein sequence was synthesized using rice-preferred codons followed by the introduction of a strong endosperm-specific promoter, Gtl3a. In addition, a signal peptide was introduced to target the Osr2HN protein into storage vacuoles (Fig. 1*B*). To enhance the solubility and stability of Osr2HN and OsrHN, the intravirion and transmembrane regions were deleted during the plasmid construction. An outline for the process of Osr2HN from transgenic rice is shown in *SI Appendix*, Fig. S1. A total of 101 positive transgenic lines were obtained using *Agrobacterium*-mediated transformation.

Osr2HN in transgenic seeds was analyzed by sodium dodecyl sulfate–polyacrylamide gel electrophoresis (SDS-PAGE) and western blot. In this study, a nontransgenic rice line of TP309 acted as a negative control. Compared with TP309, predominant protein bands of 120 and 60 kDa were found in the tandem HN and HN monomer transgenic grains, respectively (Fig. 1*C*). The bands were specifically recognized by antibodies against HN protein on western blot (*SI Appendix*, Fig. S2*A*). The expressed Osr2HN protein was also detected by NDV detection strips, whereas the wild-type seeds showed a negative result (*SI Appendix*, Fig. S2*B*). The expression levels of the Osr2HN protein were measured in five rice transgenic lines using a sandwich enzyme-linked immunosorbent assay (ELISA), with the purified HN protein serving as a protein standard. The results showed that the amount of Osr2HN protein present in the rice seeds ranged from 0.47 to 3.70 mg/g (Fig. 1*D*). The transgenic rice line P2-3 had the highest expression level (3.7 mg/g). To further investigate the localization of the Osr2HN protein, the subcellular localization of Osr2HN in endosperm cells of rice was examined by immune-electron microscopy (Fig.1*E*). Compared with the TP309, Osr2HN accumulated both in the type I protein body (PB-I) and type II protein body (PB-II). PB-I and PB-II are the two types of seed storage organelles in the rice seed endosperm, which could explain the significant production of Osr2HN in the transgenic line. Furthermore, the expression kinetics of Osr2HN in different generations were evaluated using ELISA. The results showed that the expression of Osr2HN remained stable across four generations (G1-G4) (Fig. 1*F*). Based on these findings, the P2-3 transgenic rice line was selected for scale-up and further study.

Soluble Osr2HN Formed Tetramers with Quadruple Epitopes. To characterize the structure of Osr2HN, pure Osr2HN protein was used in crystallization studies. The structure was resolved by molecular replacement using the previously determined HN structure as a template (PDB ID code 3t1e). The resolution range of the Osr2HN structure was 1.937 to 1.87 with a P21

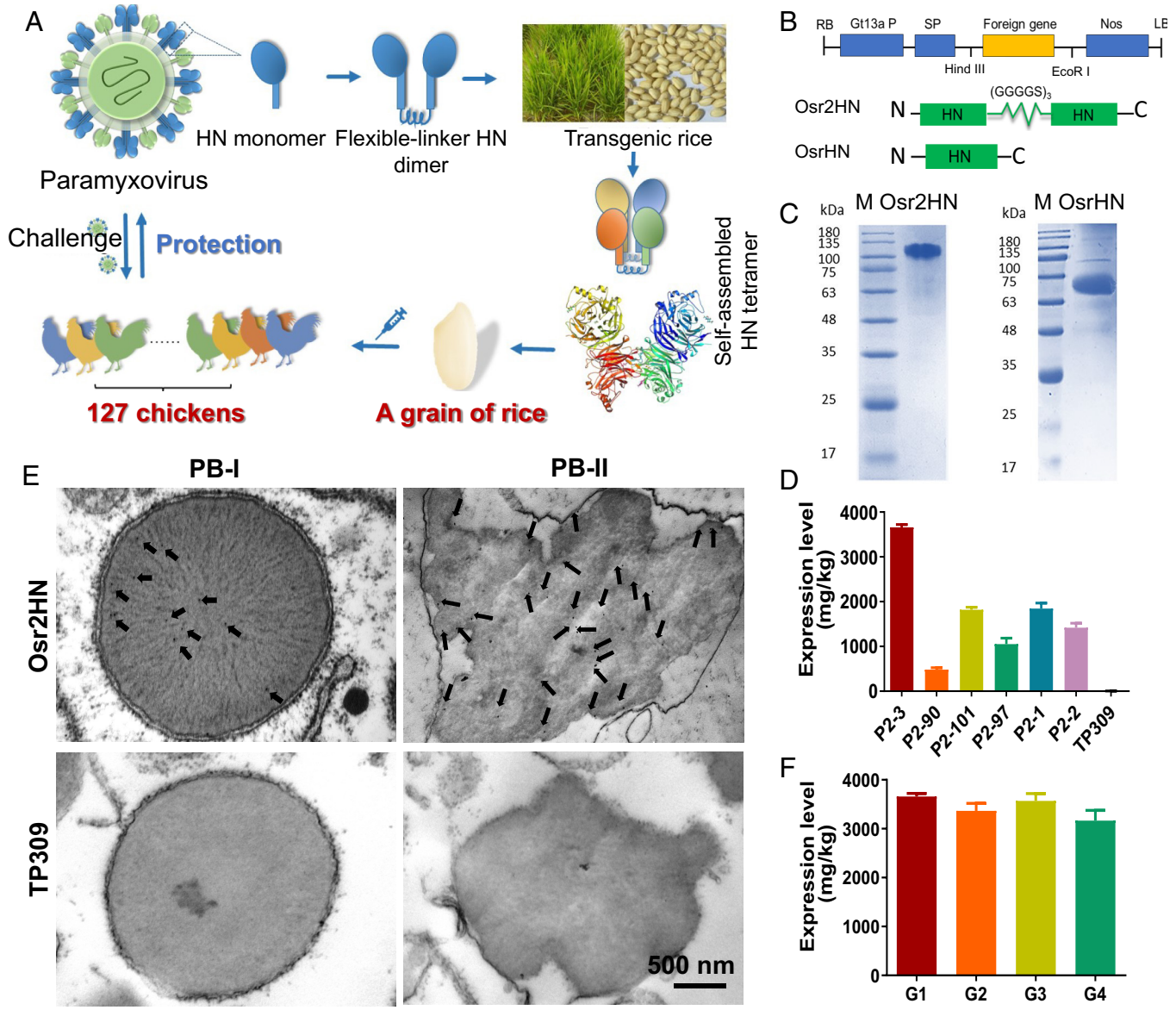

Fig. 1. Genetic construction and detection of Osr2HN. (*A*) Schematic diagram of antigen design for Osr2HN vaccine. A head-to-tail antigen model was proposed to form HN tetramers and mimic the natural structure of the major protective antigen (HN protein) in paramyxovirus. This design facilitates the formation of HN tetramers and epitope exposure, providing enhanced protection. (*B*) Schematic of pCAMBIA 1300-2HN plasmid. RB, right border; Gt13a promoter, rice seed storage protein glutelin gene promoter; SP, Gt13a signal peptide; Nos, nopaline synthase gene terminator; LB, left border; Osr2HN, two HN linked by $(GGGGS)_3$. (*C*) SDS-PAGE analysis of Osr2HN and OsrHN expressed in rice seeds. (*D*) Expression level of Osr2HN in different transgenic lines (P2-3, P2-90, P2-101, P2-97, P2-1, and P2-2) and the nontransgenic control (TP309). Mean values from three independent experiments are shown, with error bars representing SD. (*E*) Subcellular localization of Osr2HN in rice endosperm cells was detected using anti-HN antibody staining. (*F*) Stable expression of Osr2HN in transgenic line P2-3. G1, G2, G3, and G4 are the first, second, third, and fourth generations of P2-3, respectively.

21 21 space group, where the overall R-free value was 0.2359 (*SI Appendix*, Table S1). The results showed four HN molecules in one asymmetric unit of the crystal (Fig. 2*A*). The structure of each HN molecule in Osr2HN was well aligned with the HN monomer expressed in insect cells and in the human embryonic kidney cells of 293T. The RMSD values were 0.525 (PDB ID: 3t1e) and 0.504 (PDB ID: 4fzh) (Fig. 2*B*), respectively. The head domain of HN had a total of seven intrachain disulfide bonds to maintain structural stability (Fig. 2*C*). Moreover, an N-linked glycan was observed at asparagine residue 431 or 967 in structure. In order to determine the glycan structure, Osr2HN protein was digested and subjected to glycoproteomics analysis. It has been found that there are three types of N-glycans present at this position, all of which belong to the high-mannose-type N-glycans and contain six to seven Man residues. Interestingly, these glycan modifications are conserved between plant and mammalian glycoproteins, suggesting a low potential for adverse effects associated with Osr2HN (Fig. 2*D* and *SI Appendix*, Figs. S3–S5).

High flexibility leads to disordered accumulation of crystals, and hence, no electron clouds in the liner and the stalk region were found in the structure. In order to confirm the existence of the linker and the stalk regions, mass spectrometry was performed on the purified Osr2HN. The sequence coverage of the single detection reached 83%, completely covering all three of the domains in the HN protein (*SI Appendix*, Fig. S6). In addition, a peptide with 32 amino acids, including the C terminus of HN, the flexible linker, and the N terminus of HN, was detected in the mass spectrum analysis.

In the Osr2HN dimer structure, the first residues observed on the four HA domains (HN1, HN2, HN3, and HN4) were P76, G72, P76, and A75, respectively. As the structure shows in Fig. 2*E*, the C-terminal HN2 was in close proximity to the N-terminal

HN3 domain and N-terminal HN4 domain. This was likely due to the flexible linker designed in this study. In addition, the close distance between two cysteines of the N-terminal HN3 and HN4 domains provides the potential for the formation of interchain disulfide bonds, leading to the formation of Osr2HN dimers. The spatial arrangement of the HN domains on the front and back of Osr2HN was similar (Fig. 2 *E*, *Right*). Therefore, it is speculated that the HN tetramer was formed by both the natural interchain disulfide bond and the artificially designed flexible linker. To prove this speculation, we performed nonreducing SDS-PAGE to compare the molecular weights of Osr2HN with and without β-mercaptoethanol treatment (*SI Appendix*, Fig. S7). The results indicate that the molecular weights of Osr2HN proteins not treated with β-mercaptoethanol are larger, suggesting the involvement of disulfide bonds in the formation of Osr2HN tetramers. Based on the above, the potential arrangement pattern of HN1 to HN4 was proposed, where in HN2-linker-HN3 forms one Osr2HN, and HN1-linker-HN4 forms another Osr2HN.

Compared with the previously reported structure of the HN tetramer based on an additional cysteine in the stalk region, the Osr2HN dimer in this study had an angular deflection (60.65°) (*SI Appendix*, Fig. S8*B*) (38). This may be related to the pull of the linker between two HN monomers, but the angular deflection of Osr2HN did not affect the function. The epitope map showed that the epitopes of Ors2HN were exposed on the surface and were not blocked (Fig. 2*F*).

In order to check the HN oligomeric structures in solution, three sample concentrations of Osr2HN were analyzed by SAXS. Scattering curves were collected for each concentration at a 6-s exposure time. The results showed that Ors2HN at 3 mg/mL had no radiation damage and a high signal-to-noise ratio and therefore was selected for further analysis. For the Guinier analysis, the Guinier was selected from the 36th point, and the calculated Rg value was 33.78, while the range of sRg was 0.67 to 1.28 (*SI Appendix*, Fig. S9*A*). According to the Kratky plot, Iq^2 reached a minimum of 0.0258 for q = 0.158, indicating that the HN protein was completely folded in solution. After 3D modeling using Dammin software, the structural outline of the Osr2HN protein was obtained (*SI Appendix*, Fig. S9*D*). Comparing the Osr2HN crystal structure with the structure envelope obtained by SAXS, the structure obtained by SAXS was well-matched with the Osr2HN dimer (HN tetramer). This result indicated that the dimer–dimer structure obtained by the X-ray was not formed by crystal packing but rather is a dimer formed by the Osr2HN itself.

Osr2HN Induced More Robust Immunity Responses than OsrHN Monomer in Mice. To assess the immunogenicity of the vaccine, we conducted a study using BALB/c mice, which were divided into three groups. The experimental groups were administered two

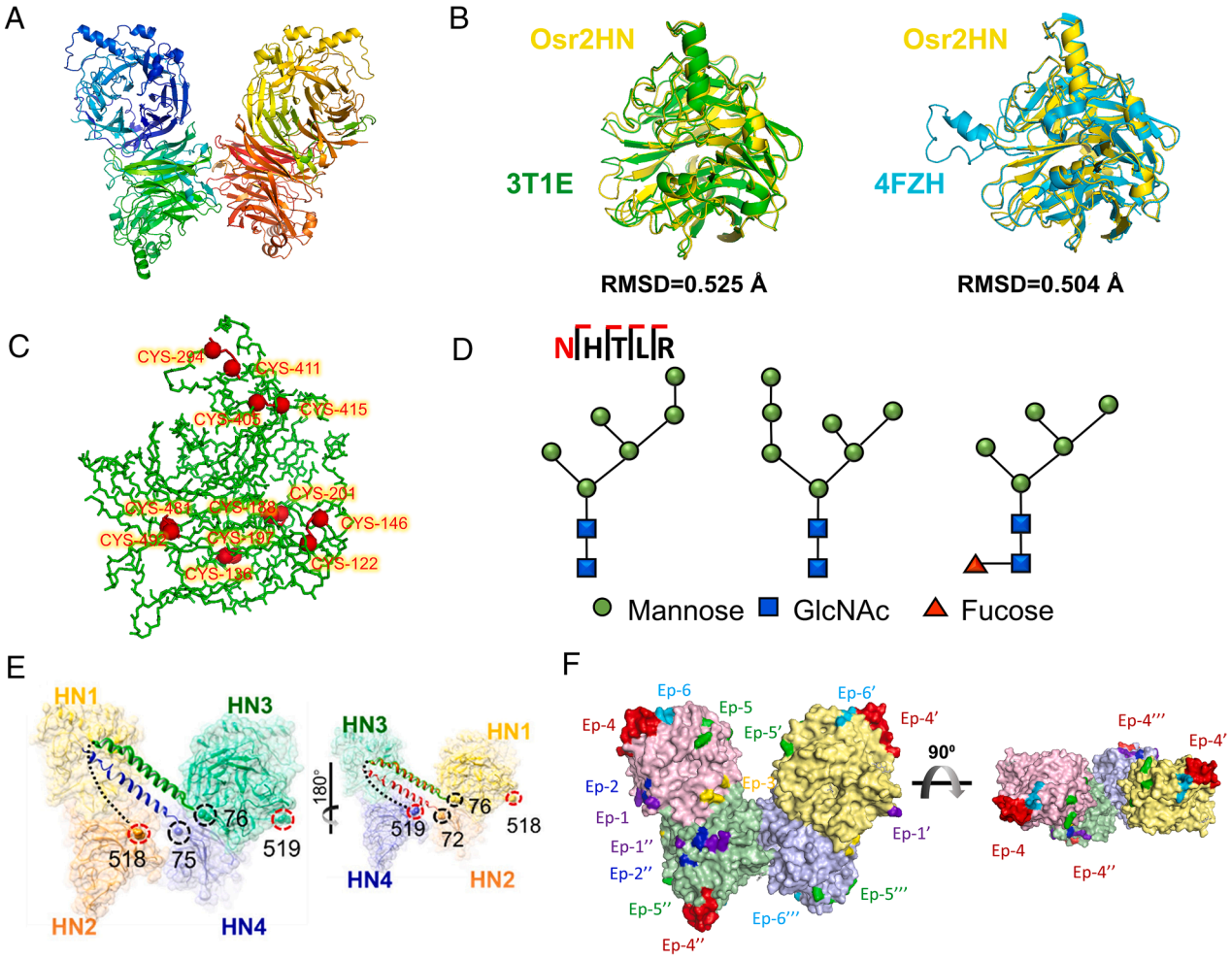

Fig. 2. Crystal structure of Osr2HN (PDB ID code 7BWU). (*A*) The overall structure of Osr2HN. (*B*) Superposition of OsrHN (yellow) with HN from insect cells (3t1e in green) and a mammalian cell expression system (4fzh in cyan). (*C*) Disulfide bond of Osr2HN. Disulfide bonds are labeled as red sticks; the cysteine forming the disulfide bonds are C122-C146, C136-C197, C188-C201, C294-C411, C405-C415, and C481-C492. (*D*) The three types of glycan structure at Asn 431 and 967 of Osr2HN (*E*) The connection between four HN domains. The black circles mark the N terminus of HN, and the red circles mark the C terminus of HN. The flexible linker between the N terminus and the C terminus is indicated by a dotted line. (*F*) The epitope map of Osr2HN. Ep1-6 are different epitopes of HN. EP, EP′, EP″, and EP‴ are the same epitopes in different HN domains.

doses of either restructured Osr2HN or OsrHN monomer, with a 21-d interval between doses. Both vaccine formulations were adjuvanted with ISA 71VG (Seppic, France). Additionally, there was a control group that received PBS with the adjuvant. Following the first immunization, we observed that restructured Osr2HN induced significantly higher titers of HN-specific antibodies in mice compared to the OsrHN monomer (Fig. 3*A*). After the booster dose was administered, antibody titers further increased in the Osr2HN group. Furthermore, we assessed the antibody subclasses in the sera on the 7th and 21st days after immunization with Osr2HN, OsrHN, and PBS with adjuvant. On the 7th day postimmunization, Osr2HN triggered significantly higher levels of IgM than the OsrHN monomer, whereas the other subclasses were present at lower levels in all groups (Fig. 3*B*). By the 21st day, class switching had occurred, with IgG1 being the predominant subclass in both Osr2HN and OsrHN groups (Fig. 3*C*). The sera of the Osr2HN group also exhibited moderate levels of IgG2, IgG3, IgG4, IgM, and low levels of IgA. However, the antibody titers of these six antibody subtypes in the Osr2HN group were higher compared to those observed in the OsrHN monomer group.

We used a panel of NDV to test the neutralizing activities of sera against NDV variants, including five strains from four different genotypes (including XX-08, F48E8, Muketeswar, ND1, and ND7). More importantly, Osr2HN induced potent and broad neutralizing antibodies against all five strains. The 100% neutralizing titer (NT100) of sera from Osr2HN groups was significantly higher than that of OsrHN (as shown in Fig. 3 *D*–*H*). These findings suggest that restructured Osr2HN exhibits superior immunogenicity compared to OsrHN. It may confer more potent and broad cross-reactive protection against NDV challenges.

Additionally, we evaluated the T cell responses induced by vaccination. After the 2nd immunization (0.5 μg), both vaccines were found to induce IL-4$^+$, IL-2$^+$, and TNF-α$^+$ CD4$^+$ T cells, with IL-4$^+$ CD4$^+$ T cells being dominant. The levels of IL-17$^+$ and IFN-γ$^+$ T cells in both groups were similar to those in the adjuvant group (Fig. 3*J*). These results suggest that both Osr2HN and OsrHN can induce a combination of Th1 and Th2 responses, with the Th2 response being more prominent. Furthermore, when comparing the Osr2HN and OsrHN groups, we observed that the Th1 and Th2 responses in the Osr2HN group were higher than those in the OsrHN group when the antigen dose was 0.5 μg. However, this difference became less pronounced when the antigen dose was increased to 10 μg (Fig. 3*K*). Additionally, we analyzed the HN-specific CD8$^+$ T cell responses in both groups. The CD8$^+$ T cell response generated by the Osr2HN vaccine was slightly stronger than that of OsrHN, but no statistically significant difference was observed between the two groups (Fig. 3*I*).

Immunogenicity of Osr2HN Vaccine in Chicken. To verify the potential of Osr2HN as a vaccine immunogen, we evaluated its immunogenicity in chickens and compare it with OsrHN and three commercial whole-virus vaccines, including the inactivated vaccine of the LaSota strain (gene II), live vaccine of the LaSota strain, and recombinant inactivated vaccine (gene A-VII) engineered by reverse genetics. All of these three commercial vaccines were produced using chicken embryo culture. The program of immunization, virus infection, and sampling is shown in Fig. 4*A*.

First, we assessed the impact of vaccine dosage on the immune response. Seven groups of SPF chickens (n = 8/group) were immunized with 0, 0.5, 1.5, 4.5, 9, 18, and 36 μg of Osr2HN protein with ISA 71VG adjuvants (Seppic, France). Sequential sera samples were collected at days 0, 5, 12, 19, and 26 postvaccination and were analyzed for hemagglutination inhibition (HI) titer. As shown in Fig. 4*B*, all of the immunized groups with six different doses developed high levels of specific HI antibodies at 12 d postimmunization. The HI antibody titers were positively correlated with immunization doses. Notably, we evaluated the antibody levels generated by the Osr2HN vaccine for up to 179 d, and it was surprising that there was no significant decline in antibody levels within 105 d after a single immunization (Fig. 4*C*). After the second immunization, the antibody titers rapidly increased and remained high levels until the end of our observation at 179 d. This suggests that the Osr2HN vaccine is capable of providing robust and sustained protection against NDV for a considerable period.

Next, we compared the immunogenicity of Osr2HN with OsrHN and three commercial whole-virus vaccines, and sera were collected weekly to detect antibody titers produced after immunization (Fig. 4*F*). Consistent with the result in mice, Osr2HN induced a more robust humoral response than OsrHN monomer with higher titers of hemagglutination-inhibiting antibodies. The group immunized with Osr2HN did not exhibit a significant decrease in antibody titers throughout the 42-d observation period, whereas the OsrHN monomer group showed a continued decline in antibody levels after 21 d. The PBS plus adjuvant group did not induce HN-specific antibodies.

Compared with three commercial whole-virus vaccines (Fig. 4 *D* and *E*), restructured Osr2HN had a distinct advantage after primary immunization, in that it produced a faster humoral immune response. In the Osr2HN group, HI antibodies could be detected on the fifth day after vaccination and reached 2^8 after 12 d of vaccination. The corresponding traditional LaSota inactivated vaccine and the LaSota live vaccine groups had no detectable HI antibodies on the 5th day after vaccination, and the antibody titers of these two commercial LaSota vaccine groups at 12 d were 2^5 and $2^{4.5}$, respectively, which were significantly lower than Osr2HN. After a booster vaccination, the antibody growth rate of Osr2HN was higher than the LaSota live vaccine group and lower than the LaSota inactivated vaccine and the A-VII inactivated vaccine group.

We also evaluated the levels of neutralizing antibodies in the serum at 28 d after two-dose immunization against three genotypes of NDV (XX-08, F48E8, and Muketeswar strains). Notably, the neutralizing titers produced by Osr2HN were comparable to the two inactivated vaccine groups and significantly higher than the HN monomer and live vaccine groups (Fig. 4 *G*–*I*). Concretely, the sera from the Osr2HN group showed a 100% neutralizing titer of $2^{10.5}$ against the homologous virus of XX-08, which was similar to the two inactivated vaccines with no significant difference ($P > 0.05$), and higher than that of the OsrHN monomer group ($2^{2.5}$) and LaSota attenuated vaccine ($2^{3.5}$). Furthermore, the Osr2HN immune sera also demonstrated potent cross-reactive neutralizing activity against the heterologous strains of F48E8 and Muketeswar. The cross-reactivity titers of Osr2HN immune sera against F48E8 and Muketeswar strains were 2^8 and $2^{9.5}$, respectively, which were significantly higher than those of OsrHN monomer ($2^{2.33}$ and $2^{2.5}$) and LaSota attenuated vaccines ($2^{4.167}$ and 2^3), was similar to that of the two inactivated vaccines ($P > 0.05$). This result indicates that the restructuring of Osr2HN elicits a broad cross-reactive neutralizing response against different genotypes of NDV.

To evaluate the T cell immunogenicity, flow cytometry was employed to quantify the HN-specific CD4$^+$ and CD8$^+$ T cell responses. The results demonstrated that a single dose of the Osr2HN vaccine elicited a moderate and balanced activation of CD4$^+$ and CD8$^+$ T cells, which were slightly higher than those induced by OsrHN and equivalent to those induced by two inactivated vaccines (Fig. 4 *J* and *K*). These findings strongly suggest

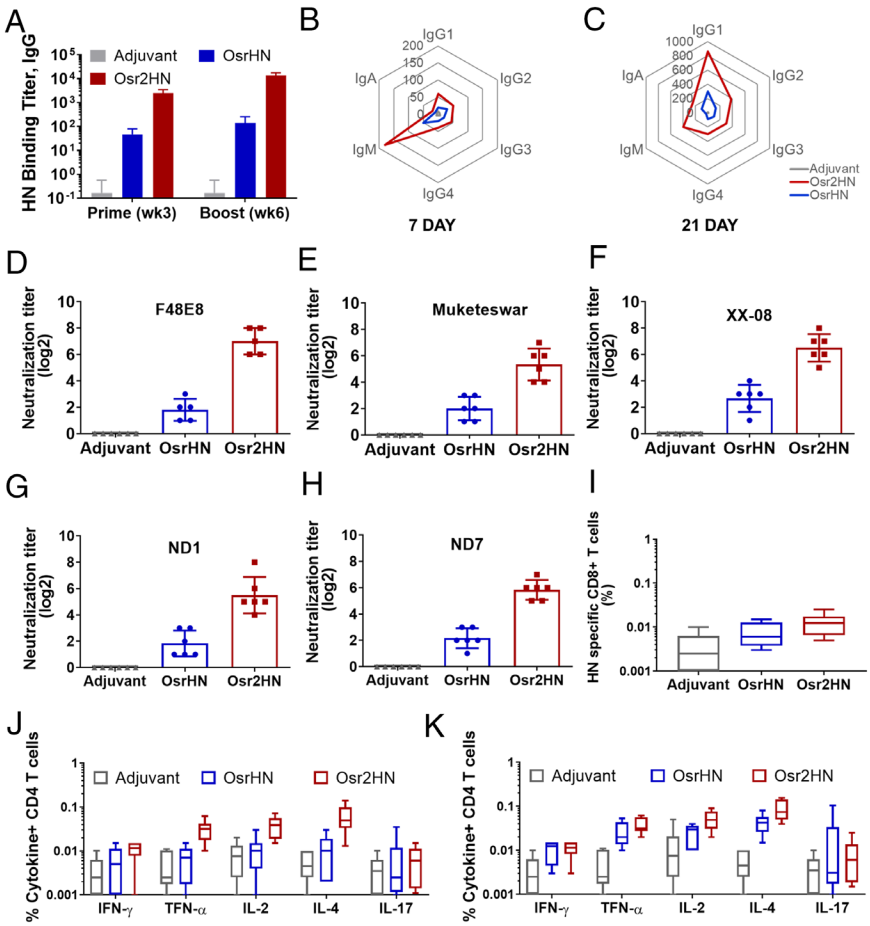

Fig. 3. Comparison of the immune responses induced by HN dimer and monomer in mice. (*A*) Antibody response induced by Osr2HN and OsrHN vaccination in mice. Serum samples were collected in the third week after the first and second immunizations and tested by the ELISA assay. Error bars indicate SEM data averaged from eight chickens per group. (*B*) Radar plot showing the Osr2HN and OsrHN induced antibody subclass at 7 d after the immunization. (*C*) Radar plot showing the Osr2HN and OsrHN induced antibody subclass at 21 d after the immunization. (*D*–*H*) Virus Neutralization assays were performed using sera from treatment groups collected on day 28 after booster immunization against five strains of NDV. The F48E8 strain is shown in (*D*), the Muketeswar strain in (*E*), the XX-08 strain in (*F*), and ND1 and ND7 strains in (*G*) and (*H*), respectively. The results displayed are representative titers from one of three independent experiments, with error bars indicating the SEM. (*I*) HN-specific $CD8^+$T cells in the blood at week 3 after boosting immunization with Osr2HN and OsrHN. (*J*) HN-specific $CD4^+$T cells in the blood at week 3 after boosting immunization with 0.5 μg Osr2HN and OsrHN. (*K*) HN-specific $CD4^+$T cells in the blood at week 3 after boosting immunization with 10 μg Osr2HN and OsrHN.

that the Osr2HN vaccine possesses the capability to stimulate both arms of the adaptive immune response.

To evaluate the safety of the vaccine, we conducted safety experiments using a high dose. Twenty-day-old chickens were given intramuscular injections of 1 mL of Osr2HN vaccine (25 μg) and 1 mL of LaSota inactivated vaccine, respectively. After a 21-d period, the chickens were dissected for analysis (*SI Appendix*, Fig. S10). The results showed that the chickens administered a high dose of the Osr2HN vaccine exhibited no signs of lesions, and the vaccine at the injection site was completely absorbed. In contrast, the chickens administered a high-dose LaSota inactivated vaccine displayed persistent redness and swelling at the injection site even after 21 d. Moreover, remnants of the vaccine, which had not been fully absorbed, were observed within the muscular layer at the injection site. Above all, these findings highlight the potential of Osr2HN as a safer and highly effective vaccine candidate for preventing and controlling NDV.

Restructuring of HN Facilitates Epitope Exposure. To evaluate the main epitopes of different vaccines, we synthesized an HN peptide library consisting of 92 peptides, named P1 to P92, with 16-mers and an offset of 6 (Fig. 5*A* and *SI Appendix*, Table S2). The peptide library contained the complete sequence of HN protein (F48E8 strain, GenBank accession No. ACK57499.1). Subsequently, we employed these peptides in the Dot-ELISA to evaluate the binding of antibodies induced by different vaccines at 21 d after boost vaccination. All positions mentioned in this part represent the locations of peptides within the full-length sequence of the HN protein. As shown in Fig. 5*B*, the regions where Osr2HN produced antibodies were on P17 to P26 (109 to 178 aa), P30 to P37 (187 to 244 aa), P41 to P58 (153 to 370 aa), and P78 to P89 (475 to 556 aa). Among them, P41 to P59 (153 to 370 aa) was the primary antigenic region, where a large number of antibodies were detected. Correspondingly, the epitope of OsrHN monomer was mainly focused on P9 to P14 (61 to 106 aa), P19 to P25 (121 to 172 aa), P53 to P54 (325 to 346 aa), and P86 to P87 (523 to 544 aa). However, the number of positive peptides was significantly fewer than that in Osr2HN. Additionally, the epitope regions of the LaSota inactivated vaccine were focused on P1 to P3 (1 to 28 aa), P9 to P25 (61 to 172aa), and P53 to P56 (325 to 358 aa). Among these, P9 to P25 (61 to 172aa) and P53 to P56 (325 to 358 aa) were identified as the primary antigenic epitope of the LaSota inactivated vaccine.

In the HN structure, the epitopes of the LaSota inactivated vaccine and OsrHN monomer were mainly located in the head of the HN protein and symmetrically distributed at the four

corners of the HN tetramer. These also included the only linear neutralizing epitope (341 to 355aa) currently identified (Fig. 5*C*). In contrast, the epitopes of the Osr2HN were not only located in the neutralizing epitope region at the four corners, similar to the inactivated vaccine and Osr2HN, but also located at the catalytic site that extends to the interface of two HN molecules in the homopolymers. Furthermore, Osr2HN also induced antibodies that recognize the peptides containing Arg 174, Arg 416, and Arg 498, as well as 198 and 236 sites. However, the sera from both the inactivated vaccine group and the OsrHN group did not exhibit the presence of specific antibodies targeting these peptides. Moreover, in comparison to Osr2HN and OsrHN, the LaSota inactivated vaccine includes B cell epitopes located in the intravirion and transmembrane regions. The presence of this epitope may be attributed to the use of the whole inactivated virus as the antigen. During the viral inactivation process, there is a possibility of disruptions to the viral structure, leading to the exposure of hidden epitopes that are not present in Osr2HN and OsrHN. However, the role of these epitopes in vaccine-induced protection remains uncertain.

Previous research has confirmed that the Arg triad in the HN protein is critical for the inhibition of NA activity, and mutations at 198 and 236 sites cause a decrease in NA and HA activities (39). The HA inhibiting activity was determined in Fig. 4 *B*–*F*. We further evaluated the NA inhibition activities of antibodies induced by three different vaccines (Fig. 5*D*). We found that the antibodies induced by the reconstructed Osr2HN exhibited higher NA inhibition titers compared to those induced by OsrHN and inactivated vaccine.

Due to the crucial roles of HA and NA activities in virus entry into and release from cells, we evaluated the neutralizing effects of three immune sera during these processes. As shown in *SI Appendix*, Fig. S11 the serum from the Osr2HN group exhibited a significantly higher capacity to inhibit virus entry into and release from BHK-21 cells compared to the OsrHN monomer group. To mitigate differences in antibody titers among the sera, we further purified the antibodies and conducted neutralization experiments using antibodies at equal concentrations (Fig. 5 *E* and *F*). Notably, the difference between the Osr2HN vaccine and the other two groups was further amplified. Specifically, at a concentration of 50 μg/mL, antibodies induced by Osr2HN completely blocked NDV infection and release from the cells, whereas antibodies induced by the OsrHN monomer only exhibited 45% and 32.5% blocking efficacy in virus infection and release, and antibodies induced by the inactivated LaSota vaccine group showed 87% and 67% blocking efficacy. These findings strongly suggest that the structural restructuring of Osr2HN enables more effective exposure of critical epitopes, leading to the generation of antibodies with higher neutralization activity.

Ultralow Dose of Osr2HN Is Sufficient to Protect Chickens against Lethal NDV Infection. We evaluated the protective efficacy of the Osr2HN vaccine using different doses and numbers of inoculations. Chickens immunized with different amounts of antigen were challenged at 28 d postvaccination with a lethal dose ($10^{6.0}$ EID_{50}) of the XX-08 strain virus by eye-dropping. Body weight and clinical presentation were monitored daily. Chickens in the PBS-mock group began to show depression, swollen eyelids, opaque eyes, and loss of appetite on the second day postinfection (dpi), and symptoms of asthma and salivation occurred at 3 dpi. Seven of the eight chickens in the nonvaccinated control group died at 4 and 5 dpi. The remaining chicken was killed due to the severity of NDV clinical signs at 7 dpi (e.g., loss of body weight >30%, severe diarrhea, and neurological signs). In contrast, all of the chickens from the vaccinated groups survived (Fig.6 *A* and *B*). Complete protection without clinical symptoms was achieved with two vaccinations at a low dose of Osr2HN (0.5 μg/dose). However, the weight of the animals in the different groups showed significant differences after challenge (Fig. 6*C*). The weight of animals in the Osr2HN group maintained rapid gain after 2 wk of challenge (mean, 13.33%), which was higher than the LaSota attenuated vaccine group (11.69%), and significantly higher than the two inactivated vaccine groups (LaSota inactivated vaccine of 3.4% and A-VII inactivated vaccine of 3.3%, $P < 0.001$). Moreover, we observed a transient increase in rectal temperature in the chickens from the inactivated vaccine groups during the 3 d after the challenge, followed by a return to normal levels. In contrast, the rectal temperature in the Osr2HN group remained stable (Fig. 6*D*). Regardless of whether the antibody titer was high or low, HN-specific antibodies in each immunized group remained stable for 15 d after the challenge (Fig. 6*E*). The anatomical results showed that the Osr2HN group had no organ damage or bleeding, while the duodenum and glandular stomach nipples of the negative group showed scattered bleeding points (Fig. 6*F*). The results of H&E staining were consistent with the anatomical results (Fig. 6*G*). In addition, some cell lysis and necrosis were observed in the spleens of animals in the negative group. In the single-dose vaccination experiment, chickens were immunized with 5 μg of Osr2HN. It was observed that all eight birds survived without displaying any symptoms during the study period following the challenge (*SI Appendix*, Fig. S12).

Discussion

Vaccines work by eliciting an immune response with consequent immunological memory that mediates protection from infection or disease (40). In 1955, some batches of polio vaccine given to the public contained the live polio virus. This case, which came to be known as the "Cutter Incident" (41), resulted in many cases of paralysis. The ideal vaccine should be safe, effective, stable, capable of large-scale production, and used in low doses. VLP vaccines have successfully improved the immunogenicity of subunit vaccines (42, 43). However, the stability and heterogeneity of particles and the problems of epitope blocking have prevented VLP from broader application. In this study, we designed a "diode" vaccine model through use of flexible linkers. The reconstituted Osr2HN protein exhibited quadruple epitopes (EP, EP′, EP″, and EP‴) that can form several different pairs and have different distances between two identical epitopes (3.26 to 12.61 nm). Appropriate distances of identical epitopes in one antigen will increase the efficacy of BCR cross-linking and B cell activation. The nano-level inoculation dose of restructured antigens completely protected animals against virus challenge, which makes the vaccine extremely safe and cheap.

In this study, HN monomers were connected by a flexible linker to form a stable dimer. Two dimers were connected by an intermolecule disulfide bond forming the HN tetramer. Yuan et al. obtained an HN tetramer structure (PDB ID: 3t1e) by introducing a cysteine mutation (S92C) in the stalk region to increase the stability of the polymer (18). Compared with the structure of the HN tetramer based on an additional cysteine, the Osr2HN dimer in this study has an angular deflection (60.65°). This may be related to the pull of the linker between two HN monomers, but the angular deflection of Osr2HN does not affect the function. The epitopes of Ors2HN are exposed on the surface and are not blocked. Moreover, we identified that the reconstruction of Osr2HN enhanced the exposure of key epitopes and active sites. Compared with the inactivated whole virus and natural HN

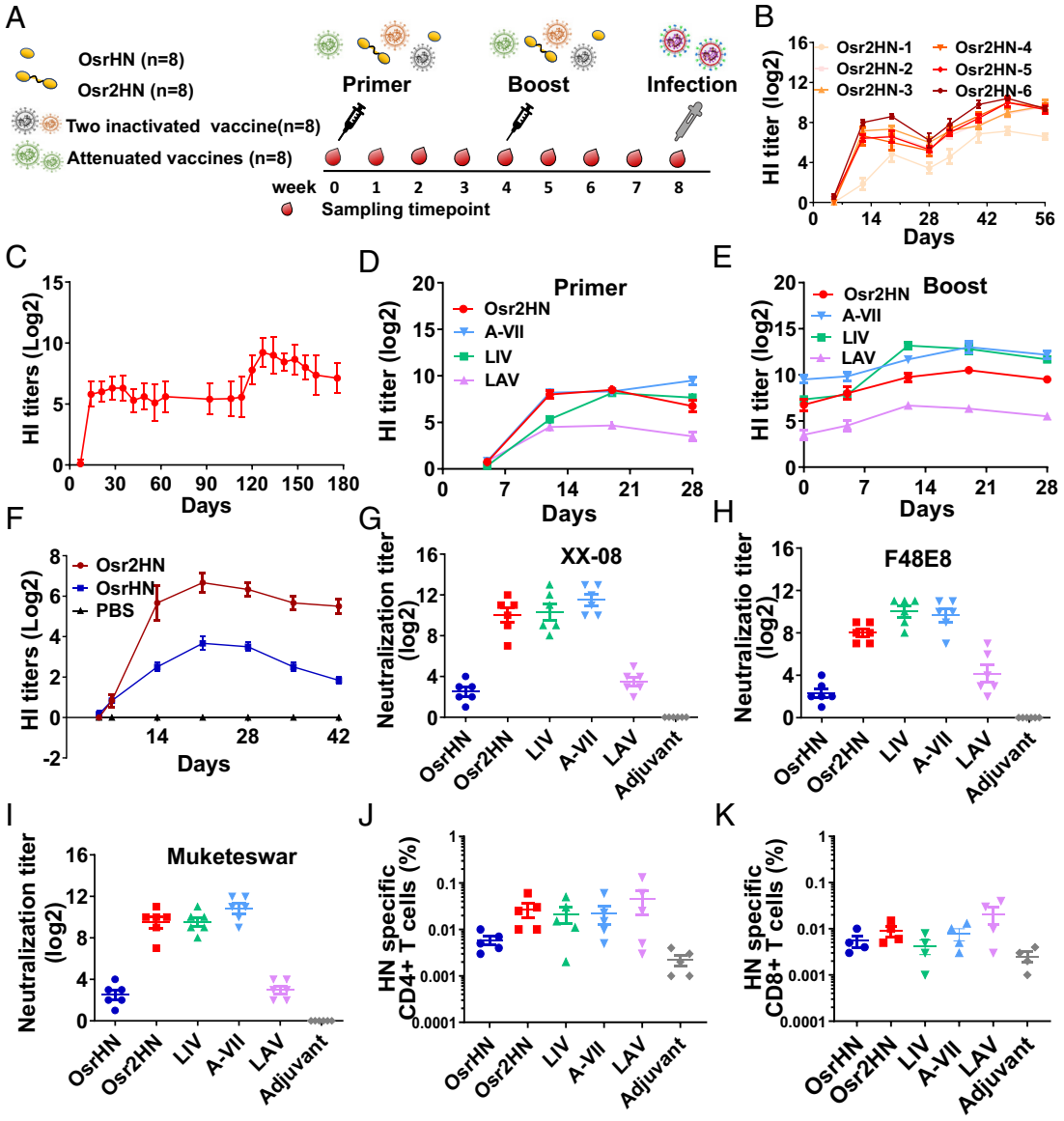

Fig. 4. Characterization of immune responses induced by Osr2HN vaccination in chickens. (*A*) Scheme of immunization, virus infection, and sampling. Chickens (n = 8) were immunized with different vaccines, including Osr2HN, OsrHN, three commercial vaccines (LIV: LaSota inactivated vaccine, A-VII: A-VII inactivated vaccine, and LAV: LaSota attenuated vaccine) as the positive controls, andTP309 with adjuvant as the negative control. At 28 d following the second immunization, animals were challenged with highly pathogenic NDV. (*B*) Chickens were immunized with different doses of the Osr2HN protein, from 0.5 μg/dose to 36 μg/dose. HN-specific antibodies were determined by the HI assay using NDV (LaSota strain). Error bars indicate SEM data averaged from eight chickens per group. (*C*) Duration of antibodies after immunization with Osr2HN. After 106 d following the first immunization, the second immunization is performed. The immunization dose is 10 μg per animal. (*D* and *E*) Comparison of antibody responses in chickens vaccinated with Osr2HN and commercial vaccines after primer immunization (*D*) and boost immunization (*E*). Data are shown as means ± SEM from six chickens. (*F*) Antibody response induced by Osr2HN and OsrHN vaccination in chickens. Error bars indicate SEM data averaged from eight chickens per group. (*G–I*) Virus neutralization assays using three genotypes of NDV (XX-08 strain, F48E8 strain, and Muketeswar strain) were performed with the sera from treatment groups sampled at day 28 after booster immunization. The results are representative titers from one of three independent experiments with error bars representing the SEM. (*J*) HN-specific $CD4^+$T cells in the blood at week 3 after boosting immunization with different vaccines. (*K*) HN-specific $CD8^+$T cells in the blood at week 3 after boosting immunization with different vaccines.

monomer, the reconstituted Osr2HN vaccine produced antibodies against the neutralizing epitope region, and also produced antibodies against both the active site and the interface of the HN homopolymer. The Arg triad (consisting of Arg 174, Arg 416, and Arg 498 sites) of the HN protein is critical for the organization of NA activity (39). Additionally, the swing of the HN head domain is crucial for the process of virus-host cell membrane fusion. This swinging action relies on the flexible loop region that connects the head and stalk domains (30, 44). The Osr2HN vaccine induces a substantial number of antibodies that recognize the interface between two HN molecules in the homopolymers, which may pose an obstacle to the swing of the head domain. Collectively, these factors contribute positively to preventing virus entry into and release from host cells.

Compared with the natural HN monomers, the reconstructed Osr2HN dimers markedly enhanced the immunogenicity of the HN protein. Consistent with this result, Gao et al. confirmed that a dimeric form of Middle East respiratory syndrome receptor-binding domains produced significantly higher neutralizing antibody titers than the conventional monomeric form. The stable dimer formed by two RBDs directly connected achieved enhancement of neutralizing antibody titers compared with the dimer formed by easily dissociated disulfide bonds (45). Compared with Gao's design, the flexible linker used in this study to form polymers

does not need to consider the flexibility and steric hindrance of the N or C termini of the protein. Moreover, this flexible linker is composed of Gly and Ser. The small sizes of these amino acids provide flexibility and allow for mobility of the connecting functional domains. The incorporation of a polar amino acid (Ser) can maintain the stability of the linker in aqueous solution by forming hydrogen bonds with water molecules. Thus, the polymer construction in this study showed no restrictions on the selection of proteins and has the possibility of a broad-scope application.

Of significance is the result that the vaccine dose was at the nanogram level by the restructuring of the HN protein. The minimum protective dose of the restructured antigen was 0.5 μg/dose, equivalent to 1/127th of a single rice seed. This amazing number indicates that Osr2HN, as a superior immunogen based on the plant expression system, will be of great value to public health. Compared to current whole-virus NDV vaccines requiring administration at levels of 10^{6-8} EID50/dose and subunit vaccines used in previous studies requiring doses over 30 μg/dose (46), the vaccination dose in our study was significantly lower due to the high immunogenicity of Osr2HN.

The plant expression system used in this study offers several advantages. Plant cultivation only requires light, water, and soil (or artificial support), making it less expensive than bioreactor kits needed for bacterial, mammalian, and insect cell culture systems (47). Additionally, the buffer solution used for Osr2HN extraction and purification is phosphate buffer containing different concentrations

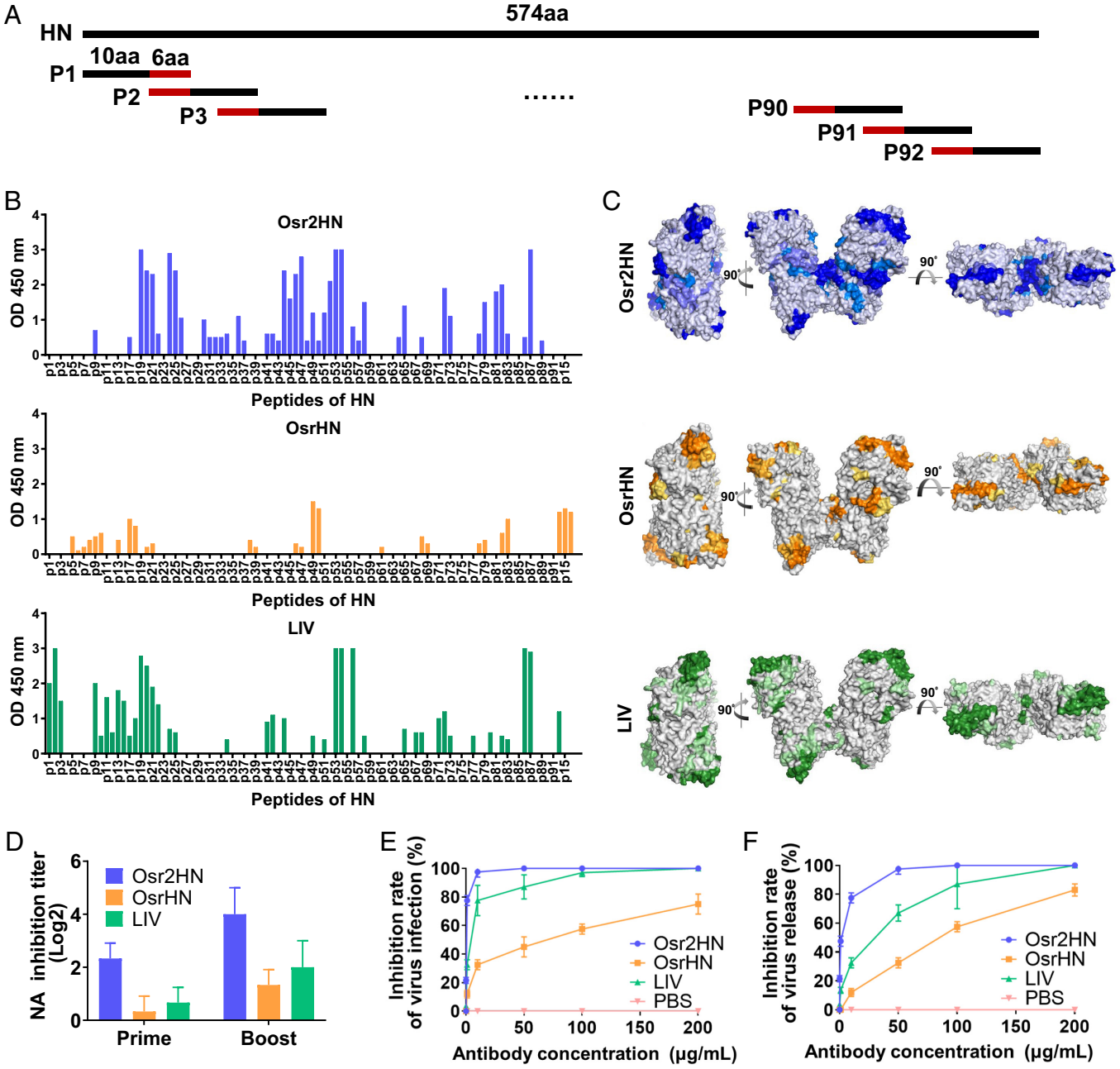

Fig. 5. Peptides map to assess antibodies of chicken after vaccination with Osr2HN, OsrHN, and LaSota inactivated vaccine. (*A*) Scheme of overlapping peptides. (*B*) Comparison of antibodies produced by the Osr2HN, OsrHN, and LaSota inactivated vaccine. (*C*) Epitope map of Osr2HN, OsrHN, and LaSota inactivated vaccine. The shade of color is positively correlated with the ELISA OD value. (*D*) The NA inhibition titer of antibody induced by the Osr2HN, OsrHN, and LaSota inactivated vaccine. (*E*) Inhibitory effects of purified antibodies induced by three vaccines on virus infection. (*F*) Inhibitory effects of purified antibodies induced by three vaccines on virus release.

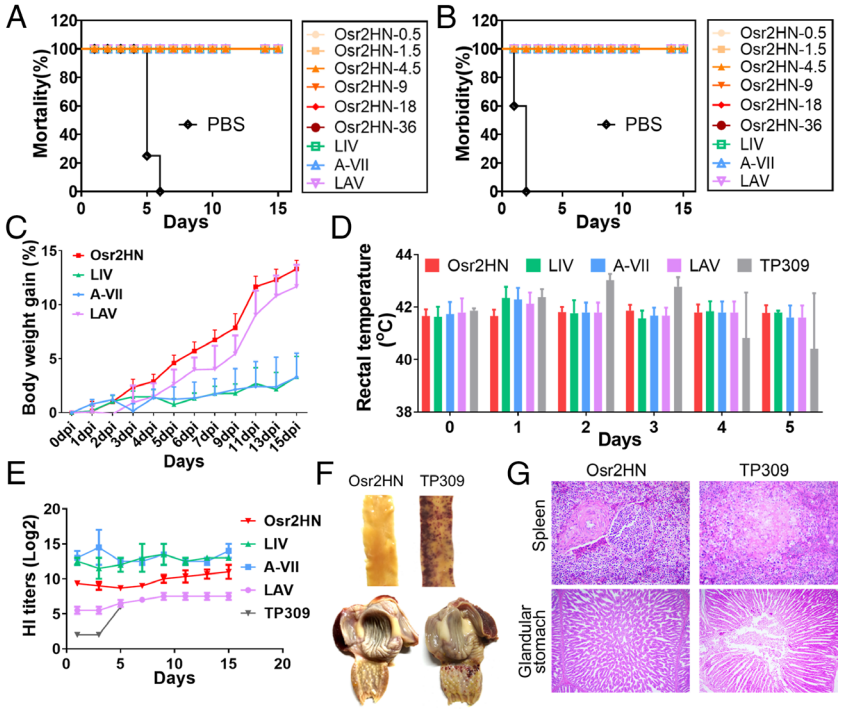

Fig. 6. Survival and clinical conditions of vaccinated chickens after challenge. (*A*) Mortality and (*B*) morbidity curves of two-dose immunization after challenge with wild-type NDV. (*C*) Weight gain of each immunization group after challenge. Error bars indicate SEM data averaged from eight chickens per group. (*D*) The rectal temperature of chickens after challenge. (*E*) HI antibody titers after challenge. Error bars indicate SEM data. (*F*) Photographs of the duodenum and stomach in different groups. (*G*) H&E staining of glandular stomach and spleen.

of NaCl, which is much cheaper than the culture medium required for cell culture systems, as well as for *Escherichia coli* and yeast culture systems. The expression level of Osr2HN in rice reached 3.7 mg/g. Although a simple comparison is not accurate, the amount of protein production is compared as mL of liquid culture equivalent to 1 g, In *E. coli* expression system, yields of HN were 0.034 to 0.37 mg/mL (48–50), with production based on the manufacturer's instruction. This expression level is lower than Osr2HN in rice. These results suggest that our system is comparable to the expression levels achieved in an *E. coli* expression system. Furthermore, transgenic rice is not susceptible to mammalian viral pathogens and plant viruses do not infect human cells. These characteristics indicate that transgenic rice seeds as bioreactors show great promise for the production of pharmaceuticals for public health at low cost and with high safety (51, 52). The vaccine platform established in this study holds the potential for supporting the United Nations Sustainable Development Goal of "no one is left behind." (53).

Rice is a highly self-pollinating crop that is a favorable host for molecular farming. The frequency of pollen-mediated gene flow is very low (0.04 to 0.08%) between genetically modified (GM) rice and adjacent non-GM plants (51, 54). This low frequency can be further decreased to negligible levels by proper spatial isolation. The field area of OsrHN transgenic rice included an isolation zone (>100 m) and a buffer zone around the field (>1.5 m). Furthermore, the standard operation protocols for planting, harvesting, and storage will largely diminish the environmental impacts. In addition, we have developed an immunochromatographic test strip for detecting the HN protein (22, 52). After soaking, rice tissue can be tested without purification to detect gene flow.

In summary, we propose a vaccine antigen model of a head-to-tail dimer through a flexible linker. Due to the precise activation of B cells, the restructured antigen completely protected chickens from lethal challenges with an ultralow inoculation dose. The extremely low dose will help to put more vaccines in one injection. In addition, the high expression level of the reconstructed antigen in rice endosperm will further reduce the cost of the vaccine and has huge market potential. More importantly, the platforms and technologies we have proposed in this study have no restrictions on the selection of proteins and have the possibility of a broad-scope application. Future studies will evaluate the immune activation mechanism of bivalent vaccines in hopes to use the model for other types of viruses.

Materials and Methods

Construction of the Plant Vector and Rice Genetic Transformation. The transgenic lines expressing Osr2HN were generated through Agrobacterium-mediated transformation. Osr2HN was purified by ion exchange chromatography and size exclusion chromatography. The expression of Osr2HN was validated by western blot and colloidal gold-based immunochromatographic strip. The details can be found in *SI Appendix*.

Immune-Electron Microscopy. Immature transgenic rice seeds were collected and fixed on day 14 after flowering. Ultrathin sections were prepared using an ultramicrotome and then treated with a mouse anti-HN antibody (dilution 1:1,000) followed by gold particle–labeled goat anti-mouse IgG (dilution 1:200). Finally, the sections were stained with uranyl acetate and imaged using a transmission electron microscope (H-7100, Hitachi, Tokyo). The detail is shown in *SI Appendix*.

The Structure Analysis of Osr2HN. The crystallized Osr2HN was obtained using a sitting drop vapor diffusion method with a precipitant solution (*SI Appendix*) and analyzed using X-ray diffraction. Manual rebuilding and structure refinement were conducted, and the final structure was visualized using PyMol. Then SAXS was employed to analyze the structure of Osr2HN in solution.

Glycoproteomics Analysis. The N-glycosylation profile of the HN protein was analyzed using mass spectrometry. Briefly, the purified Osr2HN was reduced by triethylammonium bicarbonate (TCEP) and then alkylated with iodoacetamide (IAA). Subsequently, the HN protein was digested overnight at 37 °C using trypsin.

The peptides were analyzed using C18-RPLC-MS/MS (HCD). The detailed method is described in *SI Appendix*.

Immunization Evaluation of Osr2HN in Mice and Chickens. The immunogenicity of various vaccines was assessed in BALB/c mice and SPF chickens. The plant-derived HN vaccine was prepared by mixing the purified Osr2HN, OsrHN protein with Montanide™ ISA 71 VG adjuvant (Seppic, France). The efficacy of the vaccine was evaluated by analyzing the antibody response specific to HN using the HI assay, T cell response via flow cytometry, antibody isotype determination with ELISA, and virus neutralization efficiency using the neutralization assay. The virus challenge experiment was performed on day 28 after booster immunization.

Peptides Map Assay. The primary epitopes of the different vaccines were analyzed by the peptide map assay. The peptides were synthesized and conjugated to BSA using sulfo-SMCC according to the manufacturer's instructions (*SI Appendix*) and then coated on ELISA plates at a concentration of 100 ng/well. BSA without peptides served as the negative control. The immunized sera from Osr2HN, OsrHN, and LaSota inactivated vaccine were added at a dilution of 1:50. After incubation with HRP-labeled anti-chicken antibodies, the plate was read using a microplate reader at OD_{450} nm.

Ethics Statement. All of the animal experiments involved in this study were carried out under the approval of the Animal Experimental Committee of the Henan Academy of Agricultural Sciences. All of the animals received humane care according to the Chinese animal ethics procedures and guidelines.

Data, Materials, and Software Availability. All study data are included in the article and/or *SI Appendix*.

ACKNOWLEDGMENTS. We are grateful to Professor Hongde Liang of Henan Agricultural University for his help in observing the pathological sections. We owe a debt of gratitude to the BL19U2 and BL17U1 beamlines at the Shanghai Synchrotron Radiation Facility. This work was supported by grants from the major Scientific and Technological Projects of Henan Province (221100110600), as well as the key scientific and technological projects of Henan Province (222102110210).

Author affiliations: [a]International Joint Research Center of National Animal Immunology, College of Veterinary Medicine, Henan Agricultural University, Zhengzhou 450046, China; [b]School of Advanced Agriculture Sciences, Peking University, Beijing 100871, China; [c]Longhu Laboratory of Advanced Immunology, Zhengzhou 450046, China; [d]College of Life Sciences, Zhengzhou University, Zhengzhou 450001, China; [e]Chinese Academy of Sciences Key Laboratory of Nano-Bio Interface, Division of Nanobiomedicine, Suzhou Institute of Nano-Tech and Nano-Bionics, Chinese Academy of Sciences, Suzhou 215123, China; [f]School of Basic Medical Sciences, Henan University, Kaifeng 475004, China; [g]State Key Laboratory of Hybrid Rice, College of Life Sciences, Wuhan University, Wuhan 430074, China; [h]Key Laboratory of Animal Immunology, Henan Academy of Agricultural Sciences, Zhengzhou 450002, China; [i]Wuhan Healthgen Biotechnology Corp., Wuhan 430074, China; and [j]Laboratory of Structural Biology, School of Life Sciences and School of Medicine, Tsinghua University, Beijing 100084, China

Author contributions: F.M., E.Z., and G.Z. designed research; F.M., Q.X., J.O., H.Y., K.L., Y.W., X.Z., X.N., S.Z., and X.L. performed research; A.W., D.Y., Q.L., L.W., S.C., and Z.R. contributed new reagents/analytic tools; F.M., Q.X., J.G., R.L., E.Z., and G.Z. analyzed data; and F.M., L.Z., and G.Z. wrote the paper.

1. R. Rappuoli, S. Black, D. E. Bloom, Vaccines and global health: In search of a sustainable model for vaccine development and delivery. *Sci. Transl. Med.* **11**, eaaw2888 (2019).
2. R. Rappuoli, H. I. Miller, S. Falkow, Medicine. The intangible value of vaccination. *Science* **297**, 937–939 (2002).
3. R. Rappuoli, Bridging the knowledge gaps in vaccine design. *Nat. Biotechnol.* **25**, 1361–1366 (2007).
4. S. Ozawa *et al.*, Return on investment from childhood immunization in low-and middle-income countries, 2011-20. *Health Aff (Millwood)* **35**, 199–207 (2016).
5. D. A. D'Argenio, C. B. Wilson, A decade of vaccines: Integrating immunology and vaccinology for rational vaccine design. *Immunity* **33**, 437–440 (2010).
6. B. S. Graham, M. S. A. Gilman, J. S. McLellan, Structure-based vaccine antigen design. *Annu. Rev. Med.* **70**, 91–104 (2019).
7. A. S. Lauring, J. O. Jones, R. Andino, Rationalizing the development of live attenuated virus vaccines. *Nat. Biotechnol.* **28**, 573–579 (2010).
8. A. M. Arvin, H. B. Greenberg, New viral vaccines. *Virology* **344**, 240–249 (2006).
9. G. T. Jennings, M. F. Bachmann, Designing recombinant vaccines with viral properties: A rational approach to more effective vaccines. *Curr. Mol. Med.* **7**, 143–155 (2007).
10. N. Wang, J. Shang, S. Jiang, L. Du, Subunit vaccines against emerging pathogenic human coronaviruses. *Front. Microbiol.* **11**, 298 (2020).
11. S. Chen *et al.*, Precision-engineering of subunit vaccine particles for prevention of infectious diseases. *Front. Immunol.* **14**, 1131057 (2023).
12. F. Zabel, T. M. Kündig, M. F. Bachmann, Virus-induced humoral immunity: On how B cell responses are initiated. *Curr. Opin. Virol.* **3**, 357–362 (2013).
13. H. M. Dintzis, R. Z. Dintzis, B. Vogelstein, Molecular determinants of immunogenicity: The immunon model of immune response. *Proc. Natl. Acad. Sci. U.S.A.* **73**, 3671–3675 (1976).
14. M. F. Woodruff, B. Reid, K. James, Effect of antilymphocytic antibody and antibody fragments on human lymphocytes in vitro. *Nature* **215**, 591–594 (1967).
15. A. M. Avalos *et al.*, Monovalent engagement of the BCR activates ovalbumin-specific transnuclear B cells. *J. Exp. Med.* **211**, 365–379 (2014).
16. M. F. Bachmann, G. T. Jennings, Vaccine delivery: A matter of size, geometry, kinetics and molecular patterns. *Nat. Rev. Immunol.* **10**, 787–796 (2010).
17. S. Mukherjee *et al.*, Monovalent and multivalent ligation of the B cell receptor exhibit differential dependence upon Syk and Src family kinases. *Sci. Signal.* **6**, ra1 (2013).
18. L. Javidpour, A. Losdorfer Bozic, R. Podgornik, A. Naji, Role of metallic core for the stability of virus-like particles in strongly coupled electrostatics. *Sci. Rep.* **9**, 3884 (2019).
19. K. Hashemi *et al.*, Optimizing the synthesis and purification of MS2 virus like particles. *Sci. Rep.* **11**, 19851 (2021).
20. E. C. Smith, A. Popa, A. Chang, C. Masante, R. E. Dutch, Viral entry mechanisms: The increasing diversity of paramyxovirus entry. *FEBS J.* **276**, 7217–7227 (2009).
21. T. J. Ruckwardt, K. M. Morabito, B. S. Graham, Immunological lessons from respiratory syncytial virus vaccine development. *Immunity* **51**, 429–442 (2019).
22. F. Ma *et al.*, A plant-produced recombinant fusion protein-based newcastle disease subunit vaccine and rapid differential diagnosis platform. *Vaccines* **8**, 122 (2020).
23. P. Yuan *et al.*, Structure of the Newcastle disease virus hemagglutinin-neuraminidase (HN) ectodomain reveals a four-helix bundle stalk. *Proc. Natl. Acad. Sci. U.S.A.* **108**, 14920–14925 (2011).
24. R. M. Iorio *et al.*, Neutralization map of the hemagglutinin-neuraminidase glycoprotein of Newcastle disease virus: Domains recognized by monoclonal antibodies that prevent receptor recognition. *J. Virol.* **65**, 4999–5006 (1991).
25. P. A. Thibault, R. E. Watkinson, A. Moreira-Soto, J. F. Drexler, B. Lee, Zoonotic potential of emerging paramyxoviruses: Knowns and unknowns. *Adv. Virus. Res.* **98**, 1–55 (2017).
26. R. M. Iorio *et al.*, Structural and functional relationship between the receptor recognition and neuraminidase activities of the Newcastle disease virus hemagglutinin-neuraminidase protein: Receptor recognition is dependent on neuraminidase activity. *J. Virol.* **75**, 1918–1927 (2001).
27. P. Yuan, R. G. Paterson, G. P. Leser, R. A. Lamb, T. S. Jardetzky, Structure of the ulster strain newcastle disease virus hemagglutinin-neuraminidase reveals auto-inhibitory interactions associated with low virulence. *PLoS Pathog.* **8**, e1002855 (2012).
28. S. Crennell, T. Takimoto, A. Portner, G. Taylor, Crystal structure of the multifunctional paramyxovirus hemagglutinin-neuraminidase. *Nat. Struct. Biol.* **7**, 1068–1074 (2000).
29. V. Zaitsev *et al.*, Second sialic acid binding site in Newcastle disease virus hemagglutinin-neuraminidase: Implications for fusion. *J. Virol.* **78**, 3733–3741 (2004).
30. E. Adu-Gyamfi, L. S. Kim, T. S. Jardetzky, R. A. Lamb, Flexibility of the head-stalk linker domain of paramyxovirus HN glycoprotein is essential for triggering virus fusion. *J. Virol.* **90**, 9172–9181 (2016).
31. V. Zaitsev *et al.*, Second sialic acid binding site in Newcastle disease virus hemagglutinin-neuraminidase: Implications for fusion. *J. Virol.* **78**, 3733–3741 (2004).
32. J. P. Sheehan, R. M. Iorio, R. J. Syddall, R. L. Glickman, M. A. Bratt, Reducing agent-sensitive dimerization of the hemagglutinin-neuraminidase glycoprotein of Newcastle disease virus correlates with the presence of cysteine at residue 123. *Virology* **161**, 603–606 (1987).
33. Z. Hu *et al.*, Current situation and future direction of Newcastle disease vaccines. *Vet. Res.* **53**, 99 (2022).
34. J. Mayers, K. L. Mansfield, I. H. Brown, The role of vaccination in risk mitigation and control of Newcastle disease in poultry. *Vaccine* **35**, 5974–5980 (2017).
35. Q. Zhu, J. Tan, Y. G. Liu, Molecular farming using transgenic rice endosperm. *Trends Biotechnol.* **40**, 1248–1260 (2022).
36. Y. Ogo, K. Ozawa, T. Ishimaru, T. Murayama, F. Takaiwa, Transgenic rice seed synthesizing diverse flavonoids at high levels: A new platform for flavonoid production with associated health benefits. *Plant Biotechnol. J.* **11**, 734–746 (2013).
37. Y. He *et al.*, Large-scale production of functional human serum albumin from transgenic rice seeds. *Proc. Natl. Acad. Sci. U.S.A.* **108**, 19078–19083 (2011).
38. P. Yuan *et al.*, Structure of the Newcastle disease virus hemagglutinin-neuraminidase (HN) ectodomain reveals a four-helix bundle stalk. *Proc. Natl. Acad. Sci. U.S.A.* **108**, 14920–14925 (2011).
39. S. Crennell, T. Takimoto, A. Portner, G. Taylor, Crystal structure of the multifunctional paramyxovirus hemagglutinin-neuraminidase. *Nat. Struct. Biol.* **7**, 1068–1074 (2000).
40. F. Sallusto, A. Lanzavecchia, K. Araki, R. Ahmed, From vaccines to memory and back. *Immunity* **33**, 451–463 (2010).
41. Y. Wang *et al.*, Two mutations in the HR2 region of Newcastle disease virus fusion protein with a cleavage motif "RRQRRL" are critical for fusogenic activity. *Virol. J.* **14**, 185 (2017).
42. C. J. Gunter, G. L. Regnard, E. P. Rybicki, I. I. Hitzeroth, Immunogenicity of plant-produced porcine circovirus-like particles in mice. *Plant Biotechnol. J.* **17**, 1751–1759 (2019).
43. Q. Chen, H. Lai, Plant-derived virus-like particles as vaccines. *Hum. Vaccin. Immunother.* **9**, 26–49 (2013).
44. R. K. Plemper, M. A. Brindley, R. M. Iorio, Structural and mechanistic studies of measles virus illuminate paramyxovirus entry. *PLoS Pathog.* **7**, e1002058 (2011).
45. L. Dai *et al.*, A universal design of betacoronavirus vaccines against COVID-19, MERS, and SARS. *Cell* **182**, 722–733.e11 (2020).
46. A. Homhuan *et al.*, Virosome and ISCOM vaccines against Newcastle disease: Preparation, characterization and immunogenicity. *Eur. J. Pharm. Sci.* **22**, 459–468 (2004).
47. H. Fausther-Bovendo, G. Kobinger, Plant-made vaccines and therapeutics. *Science* **373**, 740–741 (2021).
48. N. Shahid *et al.*, E. coli expression and immunological assessment of expressed recombinant Newcastle disease virus hemagglutinin-neuraminidase protein in chickens. *Acta Virol.* **64**, 331–337 (2020).
49. M. Shafaati, M. Ghorbani, M. Mahmoodi, M. Ebadi, R. Jalalirad, Expression and characterization of hemagglutinin-neuraminidase protein from Newcastle disease virus in Bacillus subtilis WB800. *J. Genet. Eng. Biotechnol.* **20**, 77 (2022).
50. M. J. Motamedi *et al.*, Immunogenicity of the multi-epitopic recombinant glycoproteins of Newcastle disease virus: Implications for the serodiagnosis applications. *Iran. J. Biotechnol.* **16**, e1749 (2018).

51. Y. He *et al.*, Large-scale production of functional human serum albumin from transgenic rice seeds. *Proc. Natl. Acad. Sci. U.S.A.* **108**, 19078–19083 (2011).
52. J. Wu *et al.*, Oral immunization with transgenic rice seeds expressing VP2 protein of infectious bursal disease virus induces protective immune responses in chickens. *Plant Biotechnol. J.* **5**, 570–578 (2007).
53. C. E. Utazi *et al.*, Mapping vaccination coverage to explore the effects of delivery mechanisms and inform vaccination strategies. *Nat. Commun.* **10**, 1633 (2019).
54. J. Rong *et al.*, Low frequency of transgene flow from Bt/CpTI rice to its nontransgenic counterparts planted at close spacing. *New Phytol.* **168**, 559–566 (2005).